

# THE EFFECT OF THE SIGNAL PROCESSOR ON THE LINE SHAPE

T. Papp<sup>1,2\*</sup> and J. A. Maxwell<sup>1</sup>

<sup>1</sup>Cambridge Scientific, 175 Elizabeth Street, Guelph, ON, N1E 2X5, Canada,

<sup>2</sup>Institute of Nuclear Research of the Hungarian Academy of Sciences  
Bem ter 18/c Debrecen, H-4027, Hungary

## ABSTRACT

Various portions of an EDX spectral line were found to be dependent on the processor used to convert an amplified signal from an energy dispersive detector to a useable spectrum; i.e. low energy tailing, both intrinsic and noise generated, events on the shoulders of peaks, residual pileup and sum peak shapes as well as “ghost” peaks. These features were shown to be noise dependent and thus time variant, as well as rate dependent and processor dependent. Minimizing and accounting for these effects are important in reducing the errors in the deconvolution of spectra into component element contributions. This along with the associated rejected event spectrum provides the basis for a more accurate quantitative analysis. The rejected spectrum is necessary to determine the true input rate.

Will appear in Vol. 53, Advances in X-ray Analysis,

---

Cambridge Scientific, 175 Elizabeth Street, Guelph,  
ON, N1E 2X5, Canada,

Telephone: (+1) 519-780-1760

Fax: (+1) 519-780-0218

e-mail: [tibpapp@cambridgescientific.net](mailto:tibpapp@cambridgescientific.net)

website: [www.cambridgescientific.net](http://www.cambridgescientific.net)



## INTRODUCTION

In quantitative energy dispersive x-ray spectroscopy (EDXRS) and elemental analysis using solid-state detectors, obtaining the true value of the counts for each element is the first step in obtaining the elemental concentrations. There are two aspects to determining the true number of events for each element. One aspect involves counting those events lost from the spectrum, which is the subject of a different paper [Papp and Maxwell, 2010], with a shorter description presented in [Papp et al., 2009a]. The second aspect is the proper deconvolution of the spectrum in order to determine the number of characteristic x-rays contributed to the spectrum by each element. This analysis depends upon knowing the detector systems response to the characteristic x-rays of each element, which in turn depends on the spectrum of characteristic x-rays produced by each element as well as the line shape response of the detection system. It has long been recognized that the line shape response and energy resolution of the detector system can play an important role in properly deconvoluting the signal from the various elements [Campbell and Wang, 1991; Van Gysel et al., 2003]. Typically, in modeling spectra, one has to define a line shape in order to fit the model to the real data. In EDXRS this shape is usually assumed to be gaussian in nature, or voigtian if one takes into account the natural lorentzian distribution [Papp and Campbell, 1996; Campbell and Papp, 2001] of the x-ray lines and convolutes this with the assumed instrumental gaussian, with low energy tailing structures often described by the phenomenological exponential tails and plateaus of the so called hypermet function [Phillips and Marlowe, 1976], or the double exponential derived from the physics of basic electron transport [Papp, 2003]. Even if these low-energy tailing features are relatively small compared to their parent peak's counts they can be significant for elements whose peaks overlap with these features. This is especially true when you consider the dynamic range of the elemental analysis where concentrations of elements can vary from sub ppm levels up to nearly unity within the same spectrum, generating peaks whose heights can vary by as much as five or more orders of magnitude. For this reason analysts have been trying for many years to characterize their detectors response function to elemental x-rays or mono-energetic radiation in order to improve the deconvolution process.

The low energy tailing features have typically been attributed to physical features of the detector such as dead layers and incomplete charge collection (ICC) areas [Goulding, 1977]. Some portion of these low energy features, such as the escape peaks due to the escape of K or L x-rays of the detector material from the detector volume have long been recognized and taken into account. Additionally, Papp [2003] has indicated that there is an expected irreducible component due to the loss of energetic photoelectrons as well as various auger electrons into and out of the layers, e.g. electrode and crystal, which explain some part of the tailing. However, in most systems the tailing features are usually orders of magnitude larger than this minimum and it is for this reason that analysts invoke various dead layers and ICC areas to explain the line shapes. Many Monte Carlo studies have been performed with such features to try to fit the model line shape to the observed line shape [Joy, 1985; Campbell et al., 2001].

However, the one thing lacking in all of these models was the effect of the signal processing electronics on the observed line shape. This is generally understandable as it was assumed that the electronics faithfully recorded the event energy signal from the detector while removing most of the event pileups and possibly some small constant fraction of degraded events

in order to produce the cleanest possible spectrum. The analyst could take into account the losses due to pileups and proceed with the analysis.

With the advent of the CSX series of digital signal processors from Cambridge Scientific, Canada [[www.cambridgescientific.net](http://www.cambridgescientific.net); Papp et al., 2005 and 2009b], we can now see that the story is not that simple. The signal processing electronics has a much greater effect on the line shape, beyond simple peak resolution and pileup rejection, than was generally credited. The CSX processors work by digitizing the staircase signal from a reset type preamplifier, use various digital discriminators to produce two spectra, one of the normal accepted events and the other of all the rejected events. Adjusting the various discrimination levels and observing the effects on both the accepted event and rejected event spectra one can readily see that the electronics is not just a simple “black box device” for reproducing the event energy signal from the detector but instead has its own effect on the line shape and content of the accepted event spectrum and therefore the analysis. Here we will concentrate on the response observed near the edge of the peaks as well as that further removed, the low energy tailing and high energy event pileup, and not the location, shape and resolution of the peaks themselves, which will be the subject of another paper. Below we will present some of our observations with various detector systems.

## **METHODS**

For this work we will present observations on spectra using the CSX digital signal processor in various modes, sometimes alone and sometimes in simultaneous processing, done by splitting the preamplifier signal, in order to show the effect of the processing electronics on the line shape observed in the accepted spectrum.

## **THE CSX PROCESSORS**

As mentioned above, the CSX digital signal processor acts by digitizing a staircase like preamplifier signal. This digitized stream is processed by algorithms implemented on a digital signal processor chip to produce one or more spectra (usually two) of events that are downloaded to a computer for storage and analysis. Many of the details of the CSX processors, including quality of spectra, throughput rates, pileup, ease of setup etc. can be found on the website [[www.cambridgescientific.net](http://www.cambridgescientific.net)] and have been discussed in other papers [Papp et al., 2009a, 2009b, 2004 and 2005].

Different models (CSX2, CSX3, CSX4, Noise Analyzer, etc.) and modes of operation (batch mode, interactive mode (single accepted spectrum only), interactive with quality assurance mode (2 spectra - accepted events & rejected events) and interactive full report or setup mode with up to 6 spectra) allow the user various levels of functionality. The CSX2 uses 2 digital discriminators based on rise time and fast pileup rejection; the CSX3 uses three digital discriminators based on noise (proportional to the standard deviation), shape (proportional to the index of similarity) and rise time discrimination; and the CSX4 uses four digital discriminators based on noise, shape, rise time and fast pileup recognition. The most frequently used mode, interactive with quality assurance, simply produces two spectra for each measurement, a spectrum of accepted events for deconvolution and determination of peak areas and a spectrum of rejected events to act as a quality control for the given measurement as well as providing necessary information on the number and nature of the lost events that is needed for determining

the true event input rate and thus correcting the deconvoluted peak areas for lost events [Papp and Maxwell 2010; Papp et al., 2009a]. A second mode, interactive full report mode, often referred to as setup mode as it is useful for setting the discrimination levels, produces up to six spectra of events, the accepted event spectrum, the total rejected event spectrum and the spectra of events rejected solely by each discriminator alone.

Another model, the noise analyzer, can be used to show two measures of the signal noise and shape on an event-by-event level based on the noise and shape algorithms used by the CSX3 CSX4 models. It produces a spectrum of the average noise and shape parameter for each event in each channel, that is, the sum of the noise or shape measure for each event in a given channel divided by the number of events in that channel.

## LINE SHAPE OBSERVATIONS

In figure 1 we see the response of a Si(Li) detector to monochromatic Cu  $K\alpha_1$  radiation as measured by the CSX4 processor. It shows the pattern of low energy tailing that is usually assumed to be the minimal intrinsic tailing of the detector due to the loss of escape x-rays and energetic photo and auger electrons from the surface of the detector. A rate dependent pileup peak is also present along with either a small background or very much reduced pileup plateau between the parent and sum peaks. We would consider this near an ideal line shape based on the physics of transport processes between detector layers for the given detection system [Papp, 2003]. Studies using the exact same detector, but using the manufacturer's analog system, show a similar quality line shape with the exception of a larger exponential tail on the low energy side of

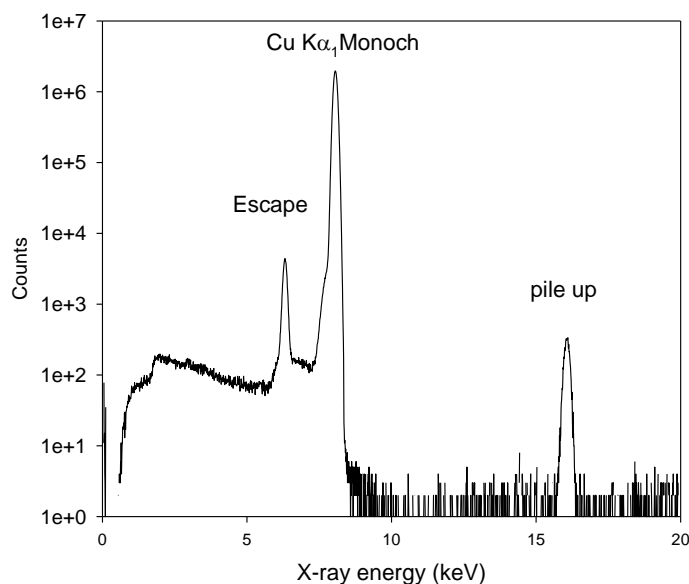


Figure 1. A spectrum of monochromatic Cu  $K\alpha_1$  x-rays collected with a Si(Li) detector and CSX4 signal processor. It shows the low energy intrinsic detector response (tailing) that is expected due to the escape x-rays and energetic photo and auger electrons.

the peak [Lepy et al., 2000].

In figure 2, we again see the results of Cu  $K\alpha_1$  radiation striking a Si(Li) detector using the CSX4 processor, but with the rejected event spectrum superposed on the accepted event

spectrum. Here we see an exponential like low energy tail in the rejected spectrum, which if present in the accepted spectrum would completely hide the intrinsic detector response as noted in figure 1. Such features, along with large low energy flat shelves, are readily observed in many recorded spectra from solid-state detector systems [Lepy et al., 2000; Eggert, 2005]. In this particular case, as is the case in many such recorded spectra, we attribute these low energy events to noise triggered events piling up with x-ray events.

Another feature that is apparent in many spectra is x-ray pileup. Piled up x-rays in the accepted spectrum have three main consequences. First, their quantity is rate dependent

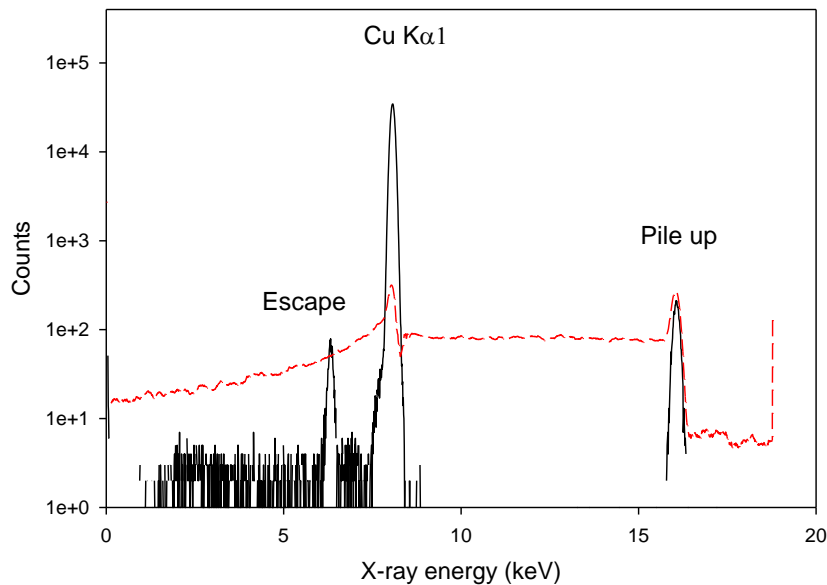


Figure 2. A spectrum of monochromatic  $\text{Cu K}\alpha_1$  x-rays collected with a Si(Li) detector and the CSX4 processor. Here the spectrum of rejected events (dashed line) overlays the spectrum. In the energy region below the peak we see the effects of noise triggered single event pileup that results in the commonly seen long range exponential tail or shelf that is much greater in magnitude relative to the peak height than the intrinsic detector tailing seen in figure 1.

imparting rate dependence to the overall line shape. Second, as can be seen in figure 3, the sum peaks may very well have a different peak structure than single event x-ray peaks of the same energy. Here we see the response of a Si(Li) detector to moderately high count rate  $^{55}\text{Fe}$  radiation. This was a simultaneous measurement; done by splitting the preamplifier signal, taken with the manufacturer's analog processor and a CSX3 signal processor. The parent peaks are similar in quality, although the CSX3 had slightly better resolution, but the pileup peak structure is greatly distorted for the analog processor versus the CSX3 processor as is readily apparent in both the 1<sup>st</sup> and 2<sup>nd</sup> order peak pileup regions. For the analog processor we see a broadening of the pileup peaks to the low energy side in the 1<sup>st</sup> order pileup region with a total loss of peak structure by second order while the CSX3 spectrum still retains the recognized peak structure one expects to see with pure sum peaks. A potential third consequence of two or more x-rays piling up is shown in figure 4. Here we show the simultaneous measurement using a Si(Li) detector with its digital signal processor and the CSX3 processor. The manufacturer's dsp shows some fast event pileup rejection but fails to suppress much of the pileup continuum between the parent and sum peaks. The CSX3 readily recognizes and provides at least 100 times better suppression

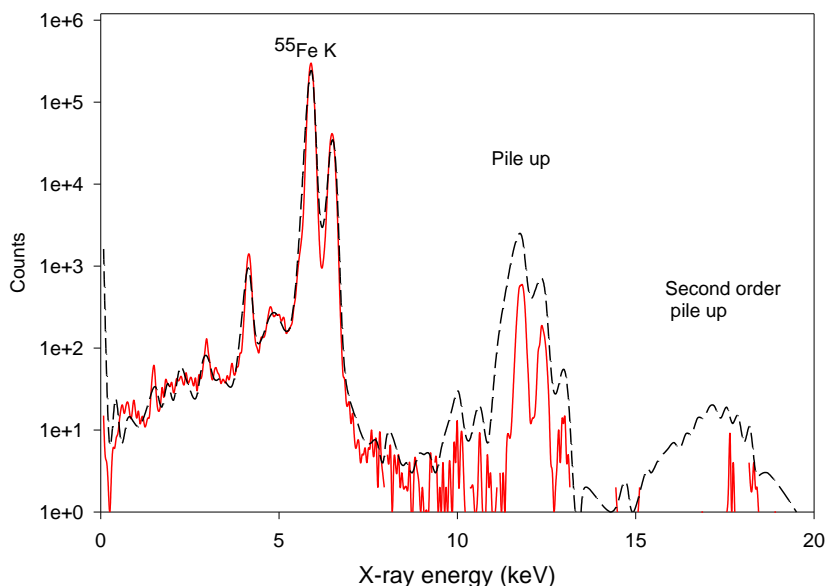


Figure 3. Spectra of  $^{55}\text{Fe}$  radiation collected with a Si(Li) detector and processed simultaneously by the manufacturer's analog electronics (black line) and a CSX3 processor (red line). We can see the effect that the processor has on the sum peak line shapes at a moderately high-count rate of 30,000 cps.

of this pileup as indicated by the difference in counts in that region (channels 600 – 800). The importance of this in a deconvolution of a complex spectrum of many elements, whose peaks might overlap these pileup event regions, is quite evident.

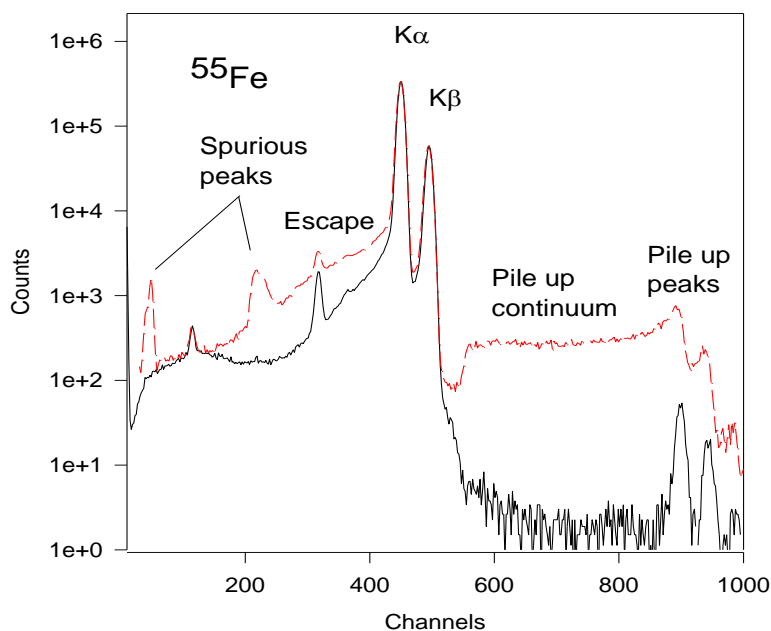


Figure 4. Spectra of  $^{55}\text{Fe}$  radiation collected by a Si(Li) detector and processed simultaneously by the manufacturer's digital signal processor setup according to instructions (red line) and a CSX3 processor (black line). We see the effect that the processor has on the residual pileup between the parent and sum peaks.

Returning to the effects of noise on the line shape, we have in addition to the long range effect of noise triggered event pileup, whose consequence can be a long low energy tail extending from the event peak down to near zero energy as seen in the rejected spectrum of figure 2, the effects on the peak shape itself in the shoulder regions.

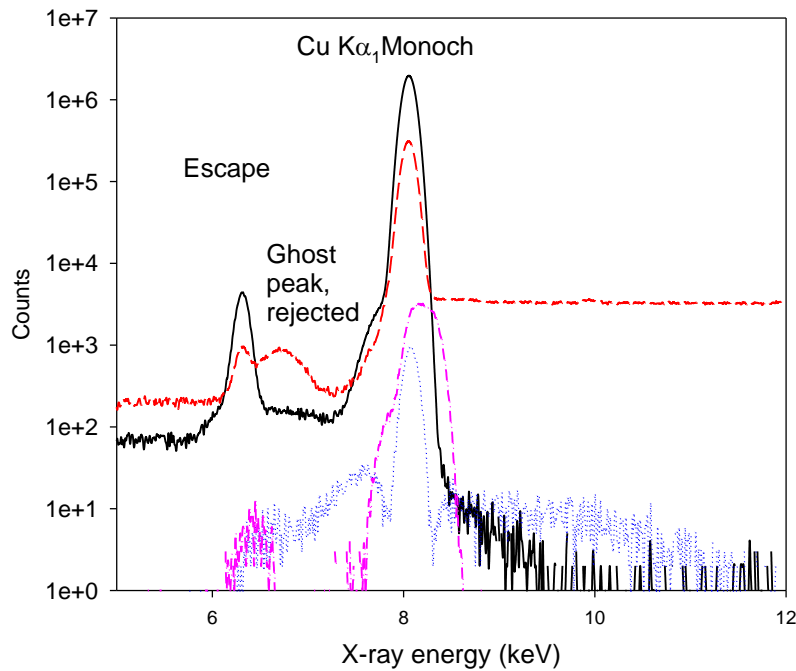


Figure 5. Spectrum of monochromatic  $\text{Cu K}\alpha_1$  radiation acquired with a Si(Li) detector and a CSX4 signal processor in setup mode shown in the region near the peak. In setup mode we see 6 spectra - 4 of which are shown superposed here, accepted (solid line), total rejected (dashed line), rejected by the fast pileup discriminator alone (dash dot line) and rejected by noise discriminator alone (dotted line). As can be seen these discriminators act to improve the quality of the line shape in the region of the peak shoulders - well below the FWHM resolution points.

On the low energy side this usually results in an increased short-range exponential tail while on the high side it results in a shoulder on the peak. These effects can be seen in figure 5 which shows  $\text{Cu K}\alpha_1$  radiation measured with a Si(Li) detector using the CSX4 signal processor in setup mode. In this mode we obtain not only the accepted and rejected spectrum but in addition the subset of events that are rejected by each of the four discriminators alone. Most of the rejected events (dashed line) are recognized by more than one of the discriminators, but some of the events near the shoulders of the peak are recognized and rejected by a single discriminator. These features are due to event-triggered pileup with noise and as such would provide a noise dependent tailing feature on both shoulders of the peak. The dash-dot line shows those events rejected by the fast pileup discriminator alone whose biggest consequence is to primarily reduce the high energy tailing but also shows some low energy tailing reduction. The dotted spectrum is that of events rejected solely by the noise discriminator and has the effect of suppressing a longer-range shoulder on both sides of the peak. Without the rejection of these noisy events the peak shape, not just resolution measured at the full width half maximum (FWHM) point, would become noise dependent effecting the overall deconvolution of the spectrum where peaks of other elements overlap these regions. Such features are often quite evident in the region between the  $\text{K}\alpha$  and  $\text{K}\beta$  lines of the lower  $Z$  ( $<30$ ) elements. This often results in analysts having to increase the low energy tailing for the  $\text{K}\beta$  complex relative to the low energy tailing of a  $\text{K}\alpha$  complex of the same energy. However, this is a wrong assignment of events as much of the surplus counts in this region of the spectrum are due to high energy tailing of the  $\text{K}\alpha$  peaks, which is not inherent to the detection system but is solely a function of the unrecognized noise.

Noise in the system can also be dependent on the energy of the event. In figure 6 we show an  $^{55}\text{Fe}$  measurement on a Si(Li) detector using the Cambridge Scientific noise analyzer. It

produces a spectrum of the event energies as before along with two additional spectra of the average noise measure and shape measure values associated with the events of each channel. For this particular detector system the average amount of noise increases with energy while the average shape measure shows no energy dependence. If the noise discriminator is not set to allow for this variation then the fraction of events rejected at each channel will change resulting in an energy dependent electronic efficiency factor that is often reported in the literature.

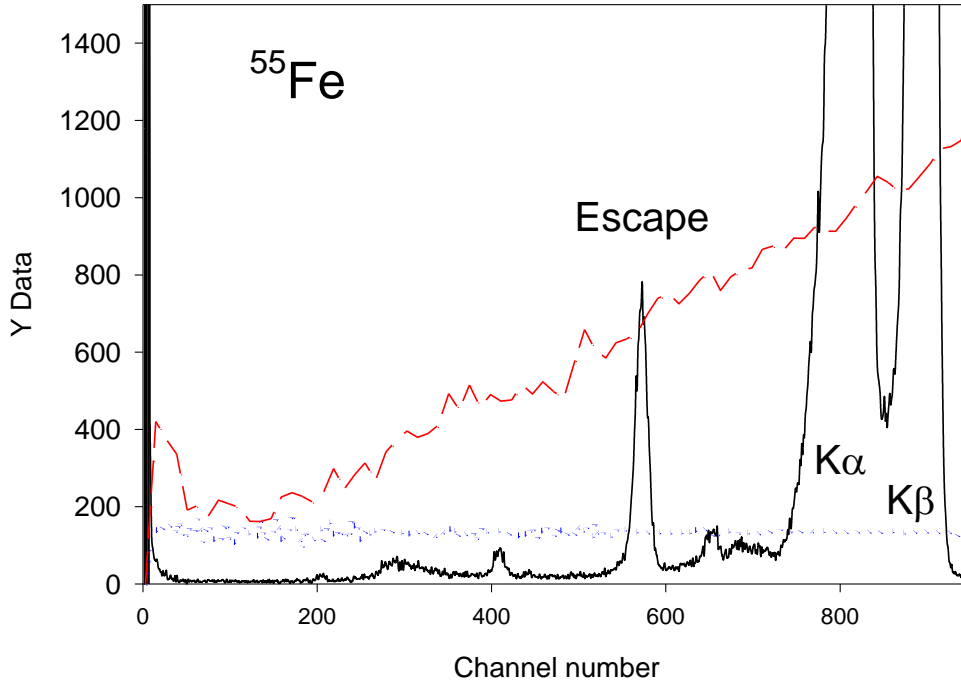


Figure 6. An expanded scale  $^{55}\text{Fe}$  spectrum taken with a Si(Li) detector and the Cambridge Scientific noise analyzer. Superposed on the spectrum (solid line) we see two measures of signal noise and shape. These measures are the average noise (dashed line) and shape measures (dotted line) for the events in each channel smoothed here for display purposes. We see that the measure of noise is energy dependent suggesting that the noise discriminator needs to be set up with similar energy dependence to avoid uneven discrimination across the spectrum or an electronic efficiency factor. In this case the shape discriminator can be set as a constant reflecting the fact that there appears to be no energy dependence of the shape measure.

Returning to figure 5, we observe a bump in the rejected spectrum between the escape peak and the parent peak for this detector. A noise analysis in this region shows a similar increase in the average noise of events in this region as is seen in figure 7. In many systems there appears a truncated shelf extending down from the peak to somewhere between 0.5 and 0.8 of the peak energy, which had been proposed earlier as originating from thermal electron out-diffusion [Papp et al., 1998; Larsson et al., 1989; Goto, 1993; Luke et al., 1994; Gartner et al., 1986; Torii et al., 1995; Goulding, 1977; Hopkinson, 1989]. The present observation may provide additional insight in finding the origin of this undesired phenomenon. In this system we see the same effect but its events have a much higher average noise value that can be discriminated against so that

the feature does not appear in the spectrum of accepted events. This suggests the possibility that with proper discrimination this artifact could be removed from many systems, as we have demonstrated for our case in the figures above.

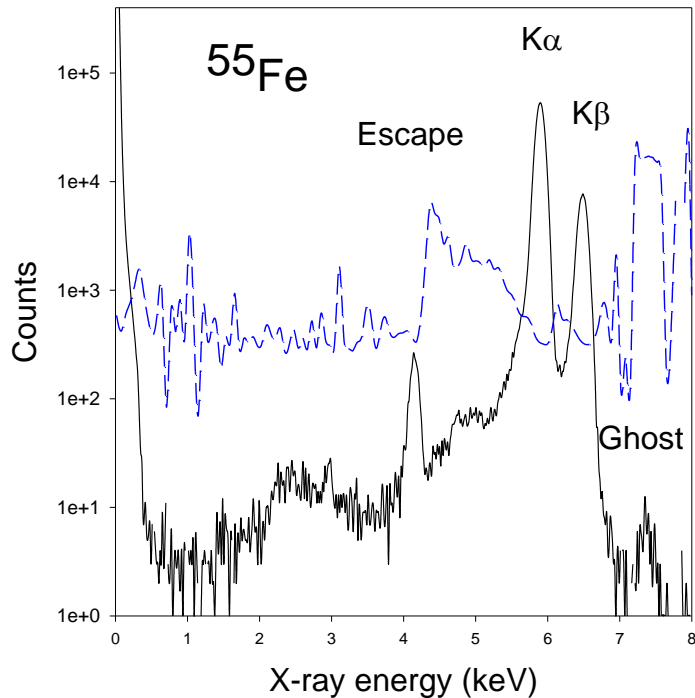


Figure 7. Again we have an  $^{55}\text{Fe}$  spectrum (solid line) acquired with a Si(Li) detector and the CSX noise analyzer. The region between the escape peak and the parent peak is populated by events with higher than average noise measure, as seen in the noise spectrum (dashed line), which can be discriminated against to improve spectral quality. This is the region where a relatively high amplitude truncated shelf is often seen with many detector systems extending from the peak down in energy to somewhere between 0.5 and 0.8 of the peak energy. Although it is present in this system as well it can be discriminated against to remove this feature from the accepted event spectrum.

Finally we will conclude by showing one other feature that is commonly seen in energy dispersive spectra, the so-called “ghost” peaks [Lepy et al., 2008]. In figure 8 we show an  $^{55}\text{Fe}$  spectrum obtained using a Si(Li) detector and a CSX3 signal processor that has been purposely left unoptimized. We see various peaks in the accepted event spectrum that cannot be explained on the basis of the source radiation. However, each of these peaks in the accepted spectrum is accompanied by a corresponding dip in the rejected spectrum indicating that while neighboring events were discriminated against that these events managed to pass the tests. As is readily seen these are mostly noise triggered single event pileups on the low energy side of the peaks and double event pileups on the high energy side. We therefore suspect that many ghost peaks are present simply because of the signal processing approach or settings. Such an example can be seen in figure 4, where the detector manufacturer’s signal processor left a peak in the region of

the Ar K lines.

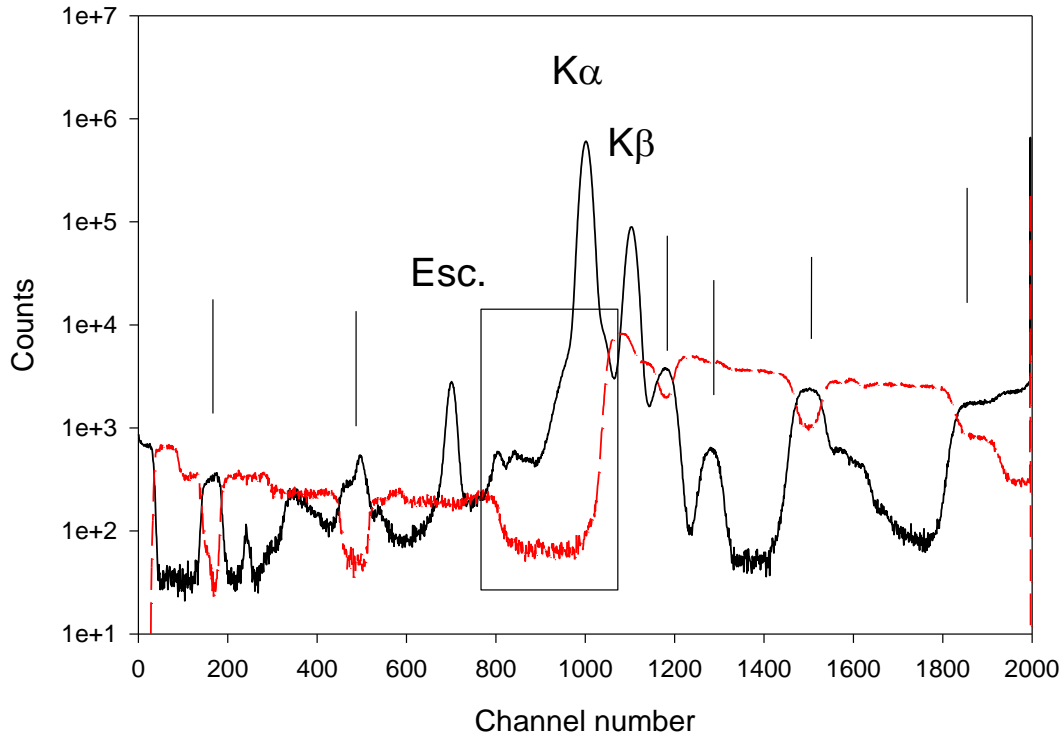


Figure 8. Here we have an  $^{55}\text{Fe}$  measurement acquired with a Si(Li) detector and a CSX3 signal processor purposely set to less than optimal conditions, i.e. discriminators levels too high. In the accepted spectrum (solid line) we see spurious or “ghost” peaks that are not present in the source radiation, and marked with vertical bars in the figure. However, we see corresponding dips in the rejected event spectrum (dashed line) that readily indicates that these are “ghost” peaks that should be removed by properly adjusting the processor. Several of the ghost peaks are marked with vertical lines and additionally the boxed region shows what happens to the accepted spectrum when noise triggered events are not recognized and removed from the spectrum resulting in greatly increased tailing in this region.

## DISCUSSION AND CONCLUSIONS

In detector modeling and experimental line shape parameterization it is customary to assume that the basic detector response is a Gaussian. We will present, in a forthcoming paper, that this assumption is not necessarily correct. We will conclude that the line shape in general is expected to be asymmetric and skewed, and that the asymmetry and skewness are strongly dependent on the x-ray energy.

In this paper we have concentrated on the non-peak line shape components of the response function. We have seen that the observed line shape depends not only on the intrinsic response of the detector but also on the processing system. The signal processor, which is

responsible for producing the best possible spectrum for analysis, effects not only the peak resolution but additionally can be responsible for effects on both the upper side of the peak such as a high energy shoulder (see figure 5), e.g. distorted sum peaks and residual pileup (see figures 3& 4), as well as enhanced effects on the low energy side both near and far from the peak (see figures 2,4,5). Attempts to characterize the line shape of the detector response function for all subsequent measurements would then depend upon having the identical conditions for all measurements, *including input rates and noise levels!*

These effects would make detector characterization a time and rate dependent process instead of a single event that is good for all times. We have seen that the response to monochromatic radiation can be spread over the entire spectrum of accepted events. When one takes into account noise triggered pileups, the intrinsic tailing due to the detector, the rate dependent pileup peaks and the residual event pileups between the parent peaks and sum peaks the fraction of events due to mono-energetic radiation that do not appear in the peak can be both significant and quite dependent on the system noise, input rate and the settings of the processing electronics. All of these factors have to be taken into account when deconvoluting a spectrum to obtain the counts due to a given element that appears in that spectrum.

The analyst does have to characterize the intrinsic, time invariant component of the line shape due to finite size of the detector that allows photons and electrons to escape and the presence of dead layers or ICC regions but has to ensure that these effects are inherent in their particular detector and not a time or rate varying function of their processor. The effects of the processor on the accepted spectrum must be either minimized or accounted for, preferably both. The analyst must work to reduce such factors as noise wherever possible, and to tune the processor to reduce the consequence of noise and rate dependence on the measurement. This will greatly reduce the errors in modeling and deconvoluting the spectrum to obtain the best measure of the counts due to each element. This combined with a proper estimation of events lost due to the finite size of the sample, intervening x-ray absorbers, the interaction efficiency of the detector and the electronic efficiency, which includes single event rejection, noise recognition, pileup measure of the lost events [Papp and Maxwell, 2010; Papp et al., 2009a], will provide a measure of the true event counts.

We conclude by simply saying that no single spectrum, even with the additional information provided by an input counter, could provide both the quality required for ease of deconvolution and analysis and the true measure of the number of x-rays of each element that interacted with the detector crystal. The signal processor approach presented here attempts to solve this issue by providing the best possible spectrum of accepted events for deconvolution and analysis while retaining the information on the lost or rejected events via the rejected event spectrum in order to distinguish between noise and real x-ray events and to provide counting corrections.

## **ACKNOWLEDGMENT**

A Marie Curie International Reintegration Grant within the 7th European Community Framework Programme supported preparation of this manuscript. One of the authors (T.P) is indebted to Prof J.L. Campbell of the University of Guelph, ON, Canada, and R.G. Lovas of Institute of Nuclear Research of the Hungarian Academy of Sciences for their encouragement and support.

## REFERENCES

- Campbell, J.L., and Papp, T. (2001). "Widths of the atomic K-N7 levels," *At. Data Nucl. Data Tables*, 77, 1-56.
- Campbell, J.L., McDonald, L., Hopman, T. and Papp, T. (2001). "Simulations of Si(Li) x-ray detector response," *X-Ray Spectrometry*, 30, 230-241.
- Gartner, R.P., Yacout, A.M., Zhang, J. and Varghese, K.(1986). "An investigation of the possible interaction mechanisms for Si(Li) and Ge detector response functions by Monte Carlo simulation," *Nucl. Instr. and Meth. A*, 242, 399-405.
- Goto, S., (1993). "Response function of a Si(Li) detector from 1 to 10 keV," *Nucl. Instr. and Meth. A*, 333, 452-457.
- Goulding, F.S. (1977). "Some aspects of detectors and electronics for x-ray fluorescence analysis," *Nucl. Instr. and Meth.* 142, 213-223.
- Larsson, N.P.-O., Tapper, U.A.S. and Martinsson, B.G. (1989). "Characterization of the response function of a Si(Li) detector using an absorber technique," *Nucl. Instr. And Meth. B*. 43, 574-580.
- Lépy, M.C., Campbell, J.L., Laborie, J.M., Plagnard, J., Stemmler, P. and Teesdale, W.J. (2000). "Experimental study of the response of semiconductor detectors to low-energy photons," *Nucl. Instr. Meth. A*, 439, 239-246.
- Papp, T. (2003) "On the response function of solid state detectors, based on energetic electron transport processes," *X-ray Spectrometry*, 32, 458-469.
- Papp, T. and Campbell, J.L. (1996) "On the accuracy of L subshell ionization cross sections for proton impact I. Spectrum fitting," *Nucl. Inst. and Meth. B* 114, 225-231.
- Papp, T. and Maxwell, J.A. (2010) "A robust digital signal processor: determining the true input rate," *Nucl. Instr. And Meth. A.*, doi:10.1016/j.nima.2009.12.002
- Papp, T., Campbell, J.L., Varga, D. and Kalinka, G.(1998). "An alternative approach to the response function of Si(Li) x-ray detectors based on XPS study of silicon and front contact materials," *Nucl. Instr. and Meth. A*, 412, 109-122.
- Papp, T., Maxwell, J.A., Papp, A., Nejedly, Z. and Campbell, J.L. (2004) "On the role of the signal processing electronics in X-ray analytical measurements," *Nucl. Inst. and Meth. B*, 219-220, 503-507.
- Papp, T., Papp, A. and Maxwell, J.A. (2005). "Quality assurance challenges in x-ray emission based analyses, the advantage of digital signal processing," *Analytical Sciences*, 21, 737-745.
- Papp, T., Maxwell, J.A. and Papp, A. (2009a). "The necessity of maximum information utilization in x-ray analysis," *X-Ray Spectrometry*, 38, 210-215.
- Papp, T., Maxwell, J.A., and Papp, A.(2009b) "A maximum information utilization approach in x-ray fluorescence analysis," *Spectrochimica Acta Part B*: 64, 761-770.
- Phillips, G.W. and Marlowe, K.W. (1976). "Automatic analysis of gamma-ray spectra from germanium detectors," *Nucl. Instr. And Meth.* 137, 525-536.
- Torii, K., Tsunemi, H., Miyata, E. and Hayashida, K. (1995). "Some characteristics of a solid state detector in the soft x-ray region," *Nucl. Instr. and Meth. A* 361, 364-371.
- Van Gysel, M., Lemberge, P. and Van Espen, P. (2003) "Implementation of a spectrum fitting procedure using a robust peak model," *X-ray Spectrometry*, 32, 434-441.
- [www.cambridgescientific.net](http://www.cambridgescientific.net), published online